論文 / 著書情報
Article / Book Information

論題	
Title	Coupled mode analysis of high-speed transverse coupled cavity vertical-cavity surface-emitting laser for low frequency chirp operations
著者	Hu Shanting, 小山 二三夫
Authors	Shanting Hu, Fumio Koyama
出典	, Vol. 18, No. 13, p. 20210239
Citation	IEICE Electronics Express, Vol. 18, No. 13, p. 20210239
発行日 / Pub. date	2021, 7
権利情報 / Copyright	本著作物の著作権は電子情報通信学会に帰属します。 Copyright(c) 2021 IEICE

IEICE Electronics Express, Vol.18, No.13, 1–5

LETTER

Coupled mode analysis of high-speed transverse coupled cavity vertical-cavity surface-emitting laser for low frequency chirp operations

Shanting Hu[1, 2, a)] **and Fumio Koyama**[2]

Abstract We demonstrate the modeling and experimental results on the modulation bandwidth and frequency chirp of the transverse coupled cavity vertical-cavity surface-emitting lasers (TCC-VCSELs). Both a 3-dB-modulation bandwidth enhancement and chirp reduction are shown in the results. These improvements could be explained by an increase in differential net gain and photon-photon resonance introduced by strong coupling in coupled cavities. Our TCC VCSEL could be useful for higher data rates and longer link lengths of single-mode fiber transmissions.

Keywords: VCSELs, laser coupling, modulators
Classification: Semiconductor Lasers

1. Introduction

A vertical-cavity surface-emitting laser (VCSEL) is the ideal optical source for supercomputers, data centers, and access/metro/core networks, in particular for short reach applications [1, 2, 3, 4, 5, 6, 7]. However, the 3 dB bandwidth, the modulation speed of semiconductor lasers is limited by relaxation oscillation frequency, parasitic capacitance, thermal effect, and so on. In our lab, we have reported the bandwidth improvement of transverse-coupled cavity (TCC) VCSELs [8, 9, 10, 11]. Enhancement of modulation bandwidth from 2×1 photonic crystal vertical-cavity surface-emitting laser arrays is reported based on the same principle [12]. Also, a hexagonal transverse-coupled-cavity VCSEL was reported for higher modulation speeds recently [13]. The bandwidth enhancement is attracting much attention for ultra-high speed direct modulations of edge emitting lasers these days [14, 15]. While the bandwidth of conventional VCSEL is 9-10 GHz, the 3 dB bandwidth of a bow-tie-shaped TCC VCSEL is increased by a factor of 3 and theoretically that chirp reduction can also be achieved due to increased differential net gain [16]. The model we used in [9, 10] based on the Lang-Kobayashi equation have restrictions in the coupling strength. Analysis of the strong coupling regime of the TCC VCSEL based on a numerical simulation was also shown in [17].

This paper introduces the modelling and characterization of bandwidth enhancement and chirp reduction of TCC VCSELs based on the coupled mode rate equations. Strong coupling regime can be simulated in the model. We present the small signal response including the bandwidth enhancement and chirp reduction dependent on the coupling parameters and the coupling phase tolerance. The bandwidth enhancement and chirp reduction can be explained by the increased frequency of carrier-photon resonance (CPR) due to detuned-loading effect [18, 19], and additionally the photon-photon resonance (PPR) at a frequency higher than CPR due to beating between different modes in coupled cavities [20, 21, 22, 23, 24, 25]. We also present a comparison between the Lang-Kobayashi model and coupled mode model. We obtained similar simulation results from the two models in low coupling strength regime. Experimental results of the bandwidth enhancement and chirp reduction are shown at the last part.

2. Structure and modelling

Figure 1 illustrates the schematic structure of our bow-tie-shaped TCC VCSEL. Two oxide-aperture-defined cavities were laterally connected. One of the square oxide apertures

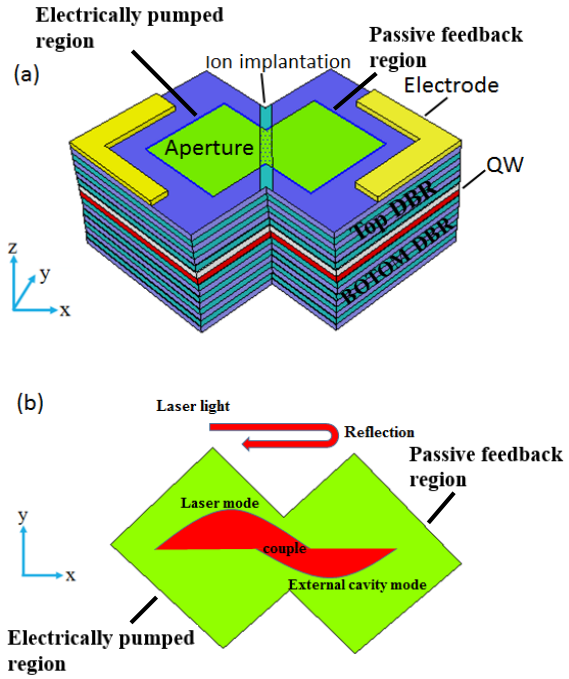

Fig. 1 Schematic structure of the TCC VCSEL

[1] Beijing University of Posts and Telecommunications, No.10 Xitucheng Road, Haidian District, Beijing, China
[2] Laboratory for Future Interdisciplinary Research of Science and Technology, Tokyo Institute of Technology, 4259 Nagatsuta, Midoriku, Yokohama 226-8503, Japan
[a)] hu.s.ab@m.titech.ac.jp

DOI: 10.1587/elex.18.20210239
Received May 27, 2021
Accepted June 3, 2021
Publicized June 11, 2021
Copyedited July 10, 2021

is operated as an electrically pumped VCSEL, while the other functions as a passive feedback cavity without an injection current. The transverse field traveled from the laser cavity to the feedback cavity through the joint region. The end interface of the feedback cavity functioned as a perfect mirror in the lateral direction, which led the lateral optical feedback into the VCSEL cavity. Strong lateral coupling between the two cavities is achieved by reducing the reflectivity and the scattering loss at the conjunction part. The coupling strength can be adjusted through changing the width of the middle of the bow. The basic idea for the bandwidth enhancement is the same as edge emitting lasers with an extended passive cavity.

Simulation of out TCC VCSEL is performed using the following coupled mode rate equations [26, 27, 28, 29, 30]. This model can be expressed by electromagnetic fields of the two coupled cavities interacting with each other through a parameter k defined as the coupling strength.

$$\frac{dS_1(t)}{dt} = \left(\Gamma_1 G_1(t) - \frac{1}{\tau_{p1}}\right) S_1(t) - 2k\sqrt{S_1(t)S_2(t)}\sin\theta, \quad (1)$$

$$\frac{dS_2(t)}{dt} = \left(\Gamma_2 G_2(t) - \frac{1}{\tau_{p2}}\right) S_2(t) + 2k\sqrt{S_1(t)S_2(t)}\sin\theta, \quad (2)$$

$$\frac{d\theta(t)}{dt} = (\omega_2 - \omega_1) - \frac{a}{2}\Gamma(G_{n2} - G_{n1}) + k\left(\sqrt{\frac{S_1(t)}{S_2(t)}} - \sqrt{\frac{S_2(t)}{S_1(t)}}\right)\cos\theta(t), \quad (3)$$

$$\frac{dN_1(t)}{dt} = \frac{\eta I_1}{qV_1} - \frac{N_1(t)}{\tau_s} - G_1(t)\,S_1(t), \quad (4)$$

$$\frac{dN_2(t)}{dt} = \frac{\eta I_2}{qV_2} - \frac{N_2(t)}{\tau_s} - G_2(t)\,S_2(t). \quad (5)$$

List of parameters used in the equations with their symbols are shown in Table I. The relative phase difference ($\theta(t)$) between the two cavities is governed by the native resonant frequency difference between two cavities as shown in Eq.(3) [31], which should be close to π for out-of-phase mode or 0 for in-phase mode. Only Eq.(1)-(4) are used since the external cavity is passive. We assume we can reduce the loss in the external cavity by increasing the detuning between lasing wavelength and bandgap wavelength of QWs.

Table I Parameters and symbols.

Parameters	Symbols
photon density in laser	$S_1(t)$
photon density in external cavity	$S_2(t)$
carrier density in laser	$N_1(t)$
carrier density in external cavity	$N_2(t)$
resonant frequency in laser	ω_1
resonant frequency in external cavity	ω_2
photon lifetime	τ_p
confinement factor	Γ
linewidth enhancement factor	a
relative phase difference	$\theta(t)$
net gain	G_n
injection current	I
current injection efficiency	η
volume of the active region	V
carrier lifetime	τ_s
nonlinear material gain	$G(t)$

3. Simulation results

Figure 2 illustrates the relationship between the coupling phase and resonant frequency difference. As we can see from the figure, larger coupling strength offers larger locking range. The coupling strength is defined by the radiated power per unit time in the lateral direction, which is dependent on the structure of the coupled cavity [32]. At the coupling strength of $0.8 \times 10^{11}\mathrm{s}^{-1}$, beyond the frequency difference 110 GHz, there is no solution to the coupling phase, indicating that the two cavity are no longer locked. The larger coupling strength of TCC VCSELs enables the locking range large enough for the modulation bandwidth enhancement. What's more, the figure also shows that as resonant frequency difference induced by gain difference and temperature difference between two cavities increases, the coupling phase deviates further from π for out of phase mode. As we presented in paper [31], a feedback phase deviated from π is needed for large bandwidth enhancement and chirp reduction. With external cavity not pumped, we can control the coupling phase through current injection in the laser cavity due to the resonant frequency difference brought by thermal effect. The asymmetric setting of current injection is needed to meet the phase condition for the bandwidth enhancement.

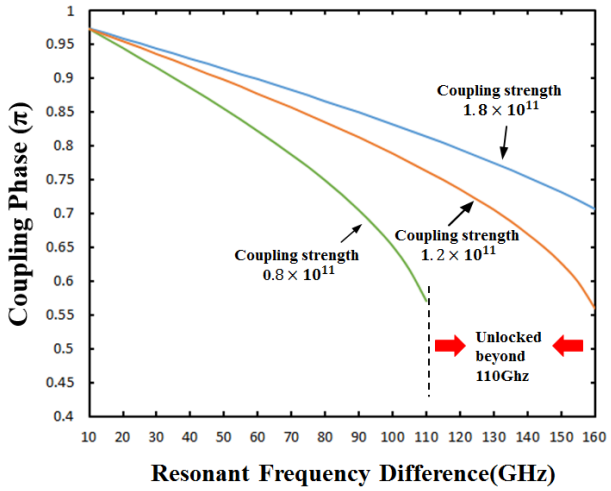

Fig. 2 Coupling phase against resonant frequency at different coupling strength.

Figure 3 (a) shows the intensity modulation response with a coupling phase of 0.75π and different coupling strengths. Stronger coupling strengths offer larger 3-dB-modulation bandwidths. The 3-dB-modulation bandwidth can be increased to 30 GHz at a coupling strength of $1.8\times10^{11}\mathrm{s}^{-1}$where we assumed the bandwidth without coupling to be only 10 GHz. According to the figure, the dent between the first CPR peak and the second PPR peak is deeper as the coupling strength increases, which limits the bandwidth enhancement brought by strong coupling. Figure 3 (b) shows the phase tolerance for the modulation bandwidth enhancement. While the bandwidth is suppressed under the in-phase condition with a feedback phase of around 0, it is increased under the out-of-phase condition with a coupling

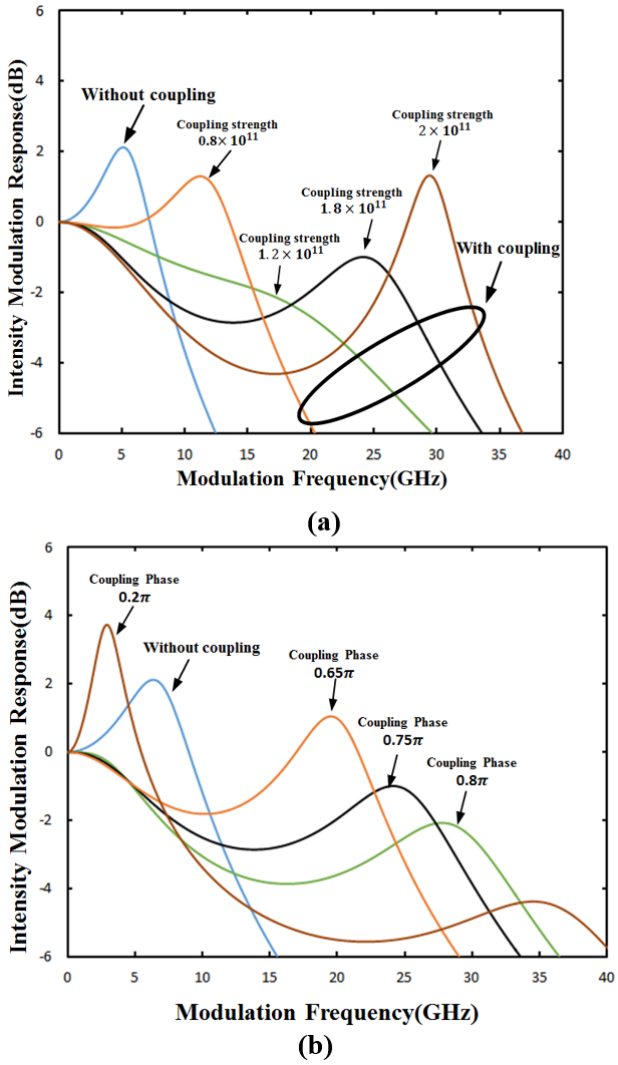

Fig. 3 (a) IM response of conventional VCSEL (blue line) and coupled cavity VCSEL at the same coupling phase and different coupling strength. (b) Phase tolerance of the modulation bandwidth enhancement

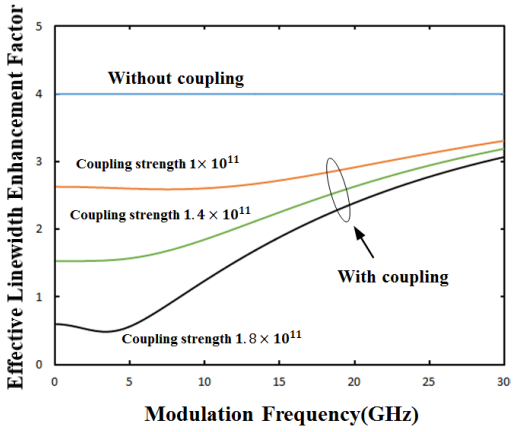

Fig. 4 Simulation results of frequency chirp as a function of modulation frequency under different coupling strength

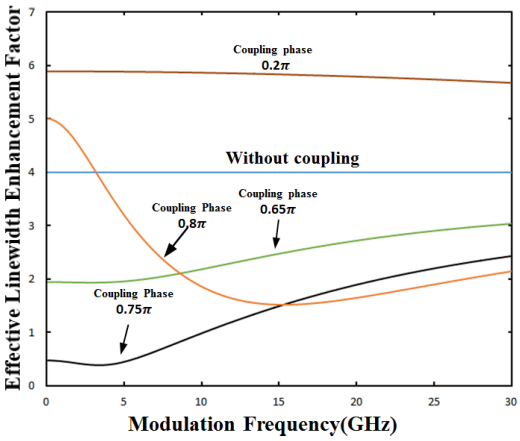

Fig. 5 Chirp reduction as a function of modulation frequency with a coupling strength of $1.8 \times 10^{11}\mathrm{s}^{-1}$.

phase of around π. These results agree with our former work [9, 16]. Also, we can see from the figure that an optimized phase offers the largest bandwidth enhancement. With coupling phase below or beyond the optimized phase, 3-dB-modulation bandwidth shrinks.

As we presented in paper [16], chirp reduction should be observed due to increased differential net gain. We expect the same simulation results in the coupled mode equation model. According to the coupled mode theory [26], the frequency of the out-of-phase mode can be written as:

$$\omega = \left(\frac{\omega_2 + \omega_1}{2}\right) + \sqrt{\left(\frac{\omega_2 - \omega_1}{2}\right)^2 + k^2}. \tag{6}$$

Using the small signal assumption and Eq. (7), we can get the chirp of the super-mode expressed by the chirp of individual modes under the basic assumption that super-mode is consisted of individual modes in each cavity.

$$\Delta\omega = \left(\frac{\Delta\omega_2 + \Delta\omega_1}{2}\right) + \frac{(\omega_2 - \omega_1)(\Delta\omega_2 - \Delta\omega_1)}{4\sqrt{\left(\frac{\omega_2 - \omega_1}{2}\right)^2 + k^2}}. \tag{7}$$

Together with Eq. (7) and coupling mode rate equations, we can calculate the effective linewidth enhancement factor by frequency-modulation intensity-modulation (FM-IM) ratio (which also can be called as the chirp-power ratio). The FM-IM ratio is used to evaluate the chirp reduction [33]. Figure 4 shows the effective linewidth enhancement factor corresponding to the parameters used in Fig. 4. The linewidth enhancement factor of a conventional VCSEL is assumed as 4. Also, an adiabatic chirp caused by nonlinear gain is neglected. Chirp reduction is clearly observed in the figure. A transient chirp can be reduced with increasing coupling strengths thanks to increased effective differential gain as explained in paper [16]. The effective linewidth enhancement factor of the coupled cavity VCSEL can be reduced below 1 at a frequency of below 10 GHz, which is almost comparable to electro-absorption modulators. Figure 5 shows the phase tolerance of chirp reduction as a function of modulation frequency with a coupling strength of $1.8 \times 10^{11}\mathrm{s}^{-1}$. While the frequency chirp is increased under the in-phase condition with a feedback phase of around 0, the bandwidth enhancement and chirp reduction can be obtained under the out-phase condition. The reduction is the largest at the optimized phase.

Figure 6 shows the comparison of the modulation bandwidth enhancement between the Lang-Kobayashi model we used before and the coupled mode model at a low coupling

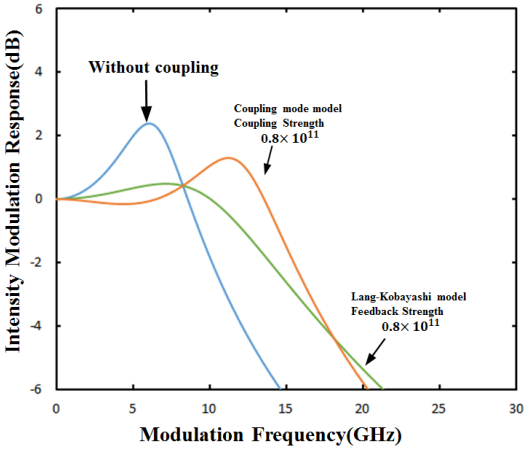

Fig. 6 Bandwidth enhancement comparison between Lang-Kobayashi model and coupled mode model.

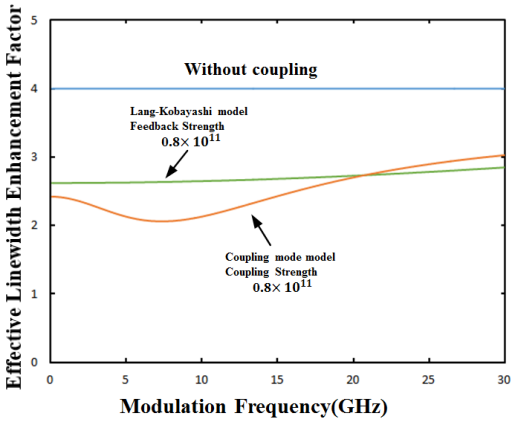

Fig. 7 Chirp reduction comparison between Lang-Kobayashi model and coupled mode model.

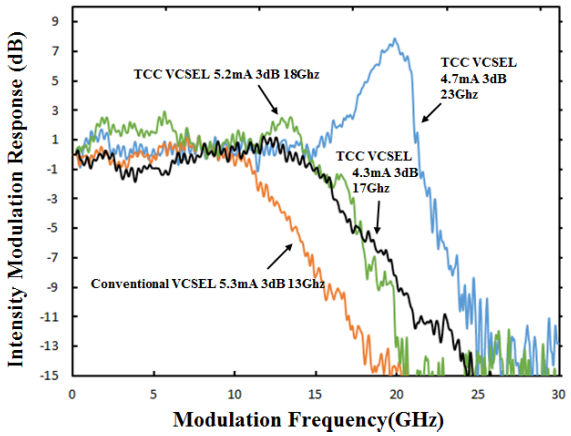

Fig. 8 Intensity modulation responses of VCSELs

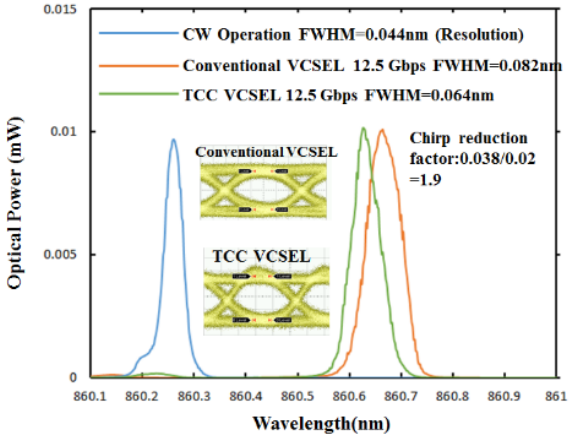

Fig. 9 Measured lasing spectra of conventional VCSEL and TCC VCSEL under 12.5 Gbps modulations

strength of $0.8 \times 10^{11} s^{-1}$ and a coupling phase of 0.75π. We can see from the figure that at the low coupling regime, the two models show almost the same 3-dB-modulation bandwidth. This result is reasonable since at low coupling strength, the increased differential gain is the main reason to increase the bandwidth. In the coupled mode model, the second peak due to PPR effect merges with the first peak at the low coupling strength, leading to a higher peak of the orange line (coupled mode model) than the green line (Lang-Kobayashi model). Figure 7 shows the comparison of the chirp reduction between the Lang-Kobayashi model and the coupled mode model. Similar simulation result is shown in the figure.

4. Experiment results

The small-signal responses of the directly modulated TCC VCSEL at different biases are shown in Fig. 8. A comparison between devices with and without feedback is shown in the figure. Without the optical feedback, a conventional VCSEL shows a maximum modulation bandwidth around 12 GHz. For the TCC-VCSEL fabricated on the same wafer, improvement of the 3-dB-modulation bandwidth up to 23 GHz is achieved at 4.7mA current pump (blue line), which is almost twice that of the conventional VCSEL. The bandwidth is also dependent on the injection current, which is because that the coupling phase and coupling strength vary by injection current change as stated in the modelling above. The coupling strength is estimated from the coupled power in a passive feedback cavity and the feedback cavity length, which is $1.66 \times 10^{11} s^{-1}$. At a bias current of 4.7mA, the calculated 3-dB-modulation bandwidth is around 25 GHz, which is close to the experiment shown in Fig. 8.

Large signal modulation and the corresponding spectrum is also measured for the conventional and TCC VCSEL respectively. As shown in Fig. 9, the net linewidth broadening is obtained by the extraction of the resolution defined by the CW spectrum (0.044nm). Under the same modulation speed (12.5Gbps), the linewidth broadening due to modulation of the conventional VCSEL (0.038nm) is almost twice that of the TCC VCSEL (0.064nm). The chirp of the TCC VCSEL is reduced by a factor of 2, which is in agreement with the simulation result.

5. Conclusion

We presented the coupled mode modeling and experimental results on the modulation bandwidth and frequency chirp of TCC VCSELs. The result shows that a TCC VCSEL can offer both bandwidth enhancement and low chirp by adjusting coupling parameters. We also compare between

the Lang-Kobayashi model and the coupled mode model in the low coupling regime. Both of the two models is in agreement with each other for a low coupling regime. Our TCC VCSEL is expected to be useful and energy cost-effective for high-speed fiber transmissions in data center and supercomputer networks.

Acknowledgments

This work is partly supported by NICT.

References

[1] M.A. Taubenblatt: "Optical interconnects for high-performance computing," J. Lightw. Technol. **30** (2012) 448 (DOI: 10.1109/jlt.2011.2172989).

[2] F. Koyama: "Recent advances of VCSEL photonics," J. Lightw. Technol. **24** (2006) 4502 (DOI: 10.1109/jlt.2006.886064).

[3] K. Iga: "Vertical-cavity surface-emitting laser: its conception and evolution," Jpn. J. Appl. Phys. **47** (2008) 1 (DOI: 10.1143/jjap.47.1).

[4] K. Iga: "Forty years of vertical-cavity surface-emitting laser: Invention and innovation," Jpn. J. Appl. Phys. **57** (2018) 08PA01 (DOI: 10.7567/jjap.57.08pa01).

[5] A. Larsson: "Advances in VCSELs for communication and sensing," IEEE J. Sel. Topics Quantum Electron. **17** (2011) 1552 (DOI: 10.1109/jstqe.2011.2119469).

[6] J.B. Jensen, *et al.*: "VCSEL based coherent PONs," J. Lightw. Technol. **32** (2014) 1423 (DOI: 10.1109/jlt.2014.2305572).

[7] A. Boletti, *et al.*: "Performance analysis of communication links based on VCSEL and silicon photonics technology for high-capacity data-intensive scenario," Optics Express **23** (2015) 1806 (DOI: 10.1364/oe.23.001806).

[8] H. Dalir and F. Koyama: "29 GHz directly modulated 980 nm vertical-cavity surface emitting lasers with bow-tie shape transverse coupled cavity," Appl. Phys. Lett. **103** (2013) 091109 (DOI: 10.1063/1.4820149).

[9] H. Dalir and F. Koyama: "High-speed operation of bow-tie-shaped oxide aperture VCSELs with photon–photon resonance," Appl. Phys. Express **7** (2014) 022102 (DOI: 10.7567/apex.7.022102).

[10] M. Ahmed, *et al.*: "Enhancing the modulation bandwidth of VCSELs to the millimeter-waveband using strong transverse slow-light feedback," Optics Express **23** (2015) 15365 (DOI: 10.1364/oe.23.015365).

[11] X. Gu, *et al.*: "850 nm transverse-coupled-cavity vertical-cavity surface-emitting laser with direct modulation bandwidth of over 30 GHz," Appl. Phys. Express **8** (2015) 082702 (DOI: 10.7567/apex.8.082702).

[12] S.T.M. Fryslie, *et al.*: "37-GHz modulation via resonance tuning in single-mode coherent vertical-cavity laser arrays," IEEE Photon. Technol. Lett. **27** (2015) 415 (DOI: 10.1109/lpt.2014.2376959).

[13] E. Heidari, *et al.*: "Hexagonal transverse-coupled-cavity VCSEL redefining the high-speed lasers," Nanophotonics **9** (2020) 743 (DOI: 10.1515/nanoph-2020-0437).

[14] S. Yamaoka, *et al.*: "Directly modulated membrane lasers with 108 GHz bandwidth on a high-thermal-conductivity silicon carbide substrate," Nature Photonics **15** (2020) 28 (DOI: 10.1038/s41566-020-00700-y).

[15] Y. Matsui, *et al.*: "Isolator-free > 67-GHz bandwidth DFB+R laser with suppressed chirp," OFC 2020 (2020) Th4A.1 (DOI: 10.1364/ofc.2020.th4a.1).

[16] S. Hu, *et al.*: "Low chirp and high-speed operation of transverse coupled cavity VCSEL," Jpn. J. Appl. Phys. **54** (2015) 090304 (DOI: 10.7567/jjap.54.090304).

[17] M. Ahmed, *et al.*: "Enhancing the modulation bandwidth of VCSELs to the millimeter-waveband using strong transverse slow-light feedback," Optics Express **23** (2012) 15365 (DOI: 10.1364/oe.23.015365).

[18] K. Vahala and A. Yariv: "Detuned loading in coupled cavity semiconductor lasers—effect on quantum noise and dynamics," Appl. Phys. Lett. **45** (1984) 501 (DOI: 10.1063/1.95316).

[19] G. Morthier, *et al.*: "Extended modulation bandwidth of DBR and external cavity lasers by utilizing a cavity resonance for equalization," IEEE J. Quantum Electron. **36** (2000) 1468 (DOI: 10.1109/3.892568).

[20] U. Troppenz, *et al.*: "40 Gb/s Directly Modulated InGaAsP Passive Feedback DFB Laser," ECOC, (2006) Th4.5.5.

[21] G.A. Wilson, *et al.*: "Modulation of phased-array semiconductor lasers at K-band frequencies," IEEE J. Quantum Electron. **27** (1991) 1696 (DOI: 10.1109/3.89995).

[22] S. Mieda, *et al.*: "Ultra-wide-bandwidth optically controlled DFB laser with external cavity," IEEE J. Quantum Electron. **52** (2016) 2200107 (DOI: 10.1109/jqe.2016.2557489).

[23] P. Bardella, *et al.*: "Design and analysis of enhanced modulation response in integrated coupled cavities DBR lasers using photon-photon resonance," Photonics **3** (2016) 4 (DOI: 10.3390/photonics3010004).

[24] P. Bardella and I. Montrosset: "A new design procedure for DBR lasers exploiting the photon–photon resonance to achieve extended modulation bandwidth," IEEE J. Sel. Topics Quantum Electron. **19** (2013) 1502408 (DOI: 10.1109/jstqe.2013.2250260).

[25] S. Sulikhah, *et al.*: "Improvement on direct modulation responses and stability by partially corrugated gratings based DFB lasers with passive feedback," IEEE Photon. J. **13** (2021) 4900214 (DOI: 10.1109/jphot.2021.3056241).

[26] M.T. Johnson, *et al.*: "Beam steering via resonance detuning in coherently coupled vertical cavity laser arrays," Appl. Phys. Lett. **103** (2013) 201115 (DOI: 10.1063/1.4830432).

[27] A. Scire, *et al.*: "Dynamics of coupled self-pulsating semiconductor lasers," IEEE J. Quantum Electron. **41** (2005) 272 (DOI: 10.1109/jqe.2004.841929).

[28] D.E. Hill: "Phased array tracking of semiconductor laser arrays with complex coupling coefficients," IEEE J. Sel. Topics Quantum Electron. **23** (2017) 1501209 (DOI: 10.1109/jstqe.2017.2701283).

[29] M. Vaughan, *et al.*: "Stability boundaries in laterally-coupled pairs of semiconductor lasers," Photonics **6** (2019) 74 (DOI: 10.3390/photonics6020074).

[30] M.J. Adams, *et al.*: "Effects of detuning, gain-guiding, and index antiguiding on the dynamics of two laterally coupled semiconductor lasers," Phys. Rev. A **95** 053869 (DOI: 10.1103/physreva.95.053869).

[31] H. Dalir and F. Koyama: "Bandwidth enhancement of single-mode VCSEL with lateral optical feedback of slow light," IEICE Electron. Express **8** (2011) 1075 (DOI: 10.1587/elex.8.1075).

[32] G. Carpintero, *et al.*: "Considerations on the rate equation description of a twin stripe laser array," Proc. SPIE 4646, (2002) 381 (DOI: 10.1117/12.470538).

[33] D. Welford: "A rate equation analysis for the frequency chirp to modulated power ratio of a semiconductor diode laser," IEEE J. Quantum Electron. **21** (1985) 1749 (DOI: 10.1109/jqe.1985.1072584).